Hamburger Beiträge
zur Angewandten Mathematik

Microscopic traffic model on the infinite line: Quasi-stationary solutions, their stability and jam waves

Bodo Werner

Nr. 2013-12
October 2013

Microscopic traffic model on the infinite line: Quasi-stationary solutions, their stability and jam waves

Bodo Werner *

October 14, 2013

Abstract

We study a very simple microscopic car following traffic model on the line with a leading car at the top, given by the ODE system

$$\ddot{x}_j(t) = \frac{1}{\tau}\Big(V(x_{j-1}(t) - x_j(t)) - \dot{x}_j(t)\Big),\ j = 2, 3, ...,$$

where $V(h)$ is a certain optimal velocity function as proposed by [BHN+95]. The leading car ($j = 1$) has no car ahead and is governed by the simple ODE

$$\ddot{x}_1(t) = \frac{1}{\tau}\Big(v_f - \dot{x}_1(t)\Big)$$

where v_f is the speed it is aiming to — the main system parameter.

This **line model** has a unique trivial solution — a quasi-stationary solution where all cars have speed v_f and headway h_f implicitely defined by $V(h_f) = v_f$. In comparison with an arbitrary infinite autocade (without a leading car), in our *leading car model* we extract a specific solution from all possible quasi-stationary solutions with constant headway h and speed v, where $v = V(h)$. The quantity $\varrho_f := 1/h_f$ can be considered as a given average traffic density on the infinite line. We are interested how ϱ_f, resp. v_f or h_f influence the traffic dynamics.

This specific quasi-stationary solution as an equilibrium of the headway-speed system is always asymptotically stable as long as we consider a finite autocade (platoon) of N cars. But already for finite autocades and certain v_f, small perturbations at the top of the autocade increase while traveling upstream and finally vanish at the end of the autocade according with the asymptotic stability of the quasi-stationary solution. Hence we conclude from numerical simulations that there are parameter regions for speeds v_f (or headways h_f or densities $\varrho_f = 1/h_f$) where the trivial solution is unstable when we consider an infinite autocade. Surprisingly the critical values seem to coincide with those for the circle model where Hopf bifurcations occur, see [SGW09], [GW10] and [Wer11]. Qualitatively, the way how the stable solutions of the line model depend on ϱ_f (or the other parameters like h_f) seems to be the same as that for the circle model (see Fig. 2) if we replace the periodic solutions bifurcating in the Hopf points by more general and partly more complex solutions which we call **jam waves**. This analogy between circle and line model includes the coexistence of stable quasi-stationary solutions with stable periodic solutions (respectively jam waves). Moreover, we discover again the *magic headways* we have found in the circle model ([Wer11]).

The main part of this paper presents results of numerical stability experiments which lead to the conjectures concerning the connection between circle and line model.

In the last part we present some theoretical approach for these conjectures. We investigate an infinite ODE system of triangular structure for which a stability concept for the trivial solutions makes sense. If we assume a principle of linearized stability we prove that the corresponding infinite matrix has continuous spectral values with positive real part where we have observed instability.

But there are several open questions, for instance concerning the type of bifurcation where jam waves seem to bifurcate from quasi-stationary solutions.

By our numerical experiments we want to stimulate some further research.

Keywords: Microscopic traffic model, infinite dynamical system, traveling waves, stability, bifurcation
AMS subject classification: 37M20, 65L07, 65P30, 65P40

*Department of Mathematics, University of Hamburg, Bundesstr. 55, 20146 Hamburg, Germany

1 Introduction

The Introduction is more detailed than usual — it is a short version of the paper.

(Loading moviehf1,3hc1,2nc10.mp4)

Figure 1: Movie: $h_f = 1.3, h_c = 1.2, n_c = 10$, see Sec. 1.2

1.1 Basic equations and results

A microscopic N-car traffic model showing an interesting bifurcation scenario consists of N identical cars on a circle was presented originally by BANDO ET AL [BHN+95], see also GASSER/WERNER([GW10]) and the references therein.
Instead of the somehow artificial **circle model** we study a much simpler N-car traffic **line model** with a leading car at the top, given by the ODE system

$$\ddot{x}_j(t) = \frac{1}{\tau}\Big(V(x_{j-1}(t) - x_j(t)) - \dot{x}_j(t)\Big),\ j = 2, ..., N \tag{1}$$

with the optimal velocity function

$$V(y) = v_{max}\frac{\tanh a(y-1) + \tanh a}{1 + \tanh a}. \tag{2}$$

The leading car No. 1 has no car ahead and is governed by the simple ODE

$$\ddot{x}_1(t) = \frac{1}{\tau}\Big(v_f - \dot{x}_1(t)\Big)$$

where v_f is the speed it is aiming to. The autocade consists of N cars and has length $L(t) := x_N(t) - x_1(t)$. Observe that the dynamics of car No. j is influenced only by its $j-1$ cars ahead.
As the circle model, this **N-car line model** has a trivial solution — a quasi-stationary solution where all cars have speed v_f and headway h_f — the most important system parameter — implicitly defined by $V(h_f) = v_f$.
This solution is an equilibrium for the headway-speed system (from now on we set $\tau := 1$)

$$\left.\begin{array}{rcl} \dot{h}_j(t) &=& v_{j-1}(t) - v_j(t), \\ \dot{v}_j(t) &=& V(h_j(t)) - v_j(t), \end{array}\right\}, \quad j = 1, 2, \ldots, N. \tag{3}$$

The line model with a finite number N of cars is extremely simple. It can be easily checked that the quasi-stationary solutions are asymptotically stable for all N, for all parameters τ, a, v_{max} and all traffic densities $\varrho_f := \frac{1}{h_f}$ (respectively for all speeds v_f of the leading car) in the usual sense that all eigenvalues of the linearisations have negative real parts. We even guess that they are the only physically reasonable limits for $t \to \infty$.
In this respect this model is boring, and this might be the reason that this simple model has not yet been in the focus of studies. But our numerical experiments show a remarkable dynamics for larger N and certain headways h_f. We show that small perturbations, for instance of the initial speed of a few cars at the top, may travel upstream and may increase in size before they vanish at the end of the autocade (according with the asymptotic stability of the quasi-stationary solution). This behavior might be related to *convective instability* (of the quasi-stationary solution) as investigated as a property of traveling waves in PDEs. The right theoretical model for the analysis of this behavior in our line model is an **infinite ODE system** like

$$\left.\begin{array}{rcl} \dot{h}_j(t) &=& v_{j-1}(t) - v_j(t), \\ \dot{v}_j(t) &=& V(h_j(t)) - v_j(t), \end{array}\right\}, \quad j = 1, 2, \ldots. \tag{4}$$

(compare (3) for a finite number of cars) which models an infinite autocade of infinite length. The concept of (asymptotic) stability and instability carries over to the quasi-stationary solution considered as an equilibrium of an infinite ODE system. Hence the quasi-stationary solution is unstable, if some small perturbation travels upstream with increasing amplitudes. We call this kind of (in)stability of the quasi-stationary solution **convective (in)stability** without presenting a rigorous definition and relation to this concept in the PDE literature.

In comparison with an infinite autocade in both directions, by our *leading car model* we extract a specific solution from all possible quasi-stationary solutions having constant headway h and speed v, where $v = V(h)$. The average traffic density is givem by $\varrho_f := 1/h_f$. We are interested in the question how ϱ_f, resp. v_f or h_f influence the traffic dynamics, especially the convective stability of the quasi-stationary solution.

In the circle model, the stability of the quasi-stationary solution depends on the headway h_f resp. on the average traffic density $\varrho_f = 1/h_f$: If $\alpha := V'(h_f) > 0.5 =: \alpha^H$, they are unstable and periodic solutions (periodic in headway and speed) arise due to Hopf bifurcation. α^H can be considered as an asymptotic Hopf parameter, since for N large enough, the quasi-stationary solutions are stable if $\alpha < \alpha^H$ (which is true for sufficiently small and sufficiently large densities). Fig. 2 shows a typical bifurcation result for the circle model. Note that the quasi-stationary solutions are unstable for $\varrho \in (\varrho_1^H, \varrho_2^H)$ and that there is a coexistence of stable quasi-periodic and stable periodic solutions (for $\varrho_1^T < \varrho < \varrho_1^H$ and for $\varrho_2^H < \varrho < \varrho_2^T$). The Hopf bifurcation at ϱ_1^H is more interesting from a practical point of view than that at the larger density ϱ_2^H. For $\tau := 1, a = 2, v_{max} = 1$ — the values in [GW10], [Wer11] and also in this paper — we get the asymptotic ($N \to \infty$) numerical values[1]

$$\varrho_1^T = 0.53 < \varrho_1^H = 0.69 < \varrho_2^H = 1.81 < \varrho_2^T = 6.94,$$

$$h_1^T = 1.8559 > h_1^H = 1.45 > h_2^H = 0.55 > h_2^T = 0.1441.$$

Fig. 3 shows a more detailed bifurcation result for $N = 40$ cars in dependence of the headway h_f which is restricted to $1.3 < h_f < 2$ to demonstrate the coexistence of stable quasi-stationary and stable periodic solutions for $h_1^H < h_f < h_1^T$. For $N = 40$ the turning point parameter $h_1^T \approx 1.72$ is still away from the asymptotic value $h_1^T = 1.8559$ for $N \to \infty$.
The main numerical result[2] presented in this paper, is that in certain respect the diagrams 2 and 3 are also true for the line model with an infinite autocade. Instead of periodic solutions (traveling waves) in the circle model we have more general **jam waves** which differ from the quasi-stationary solutions considerably. This analogy includes the coexistence of jam waves with convectively stable quasi-stationary solutions and the constant speed of the jam fronts. But in contrast to the

[1] $h_j, j = 1, 2$ are the so called *magic headways* from [Wer11].
[2] We set $\tau := 1, a = 2, v_{max} = 1$.

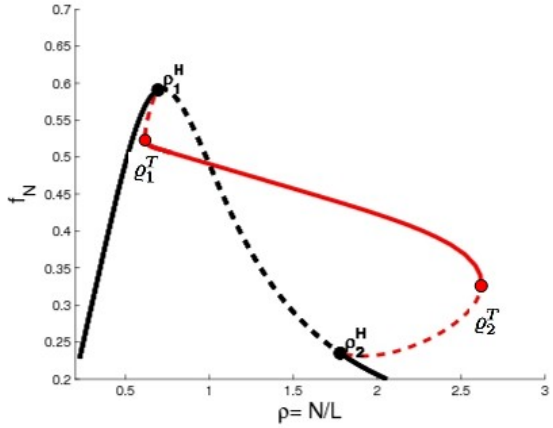

Figure 2: Solution diagram for periodic solutions on a circle of length L with 20 cars

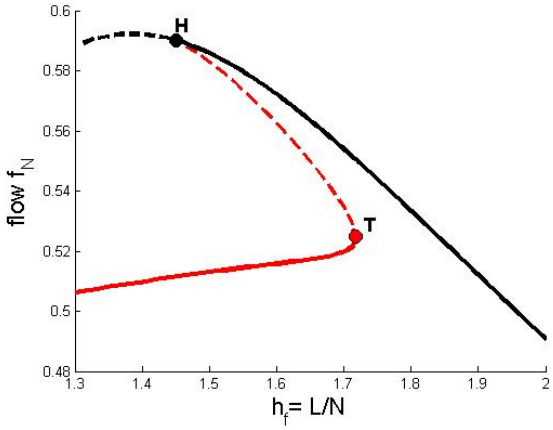

Figure 3: Solution diagram for periodic solutions on a circle of length L with 40 cars, $1.3 < h_f < 2$

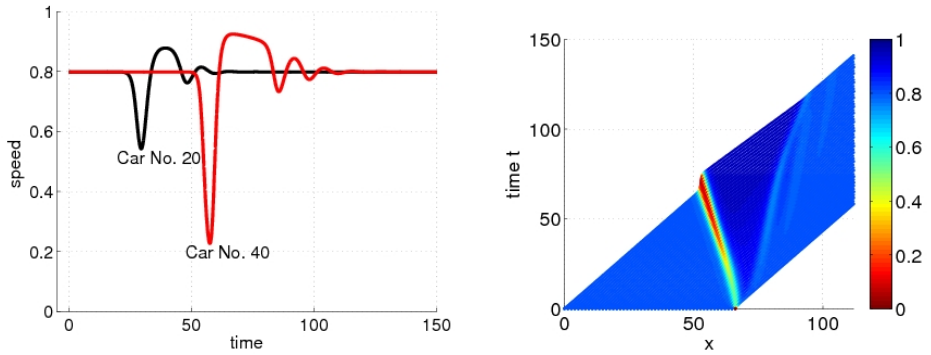

(a) Time-speed function for cars No. 20, 40 (b) Macro visualization of speed

Figure 4: Time-speed dynamics for $h_f = 1.35$ ($\varrho_f = 0.74, v_f = 0.799, \alpha = 0.65$) and $v_c = 0.27$

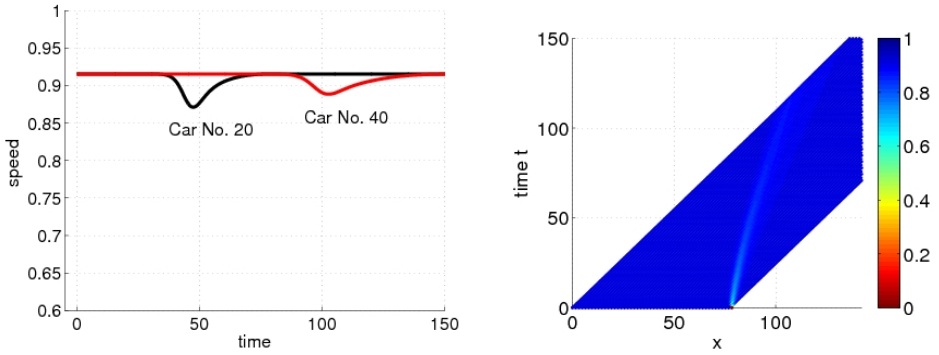

(a) Time-speed function for cars No. 20, 40 (b) Macro visualization of speed

Figure 5: Time-speed dynamics for $h_f = 1.6$ ($\varrho_f = 0.63, v_f = 0.915, \alpha = 0.31$) and $v_c = 0.31$

circle model where Hopf bifurcation occurs for $\alpha = \alpha^H$ and where we could numerically compute stable and unstable periodic solutions we do not know the character of bifurcation and we can only find (stable) jam waves by simulation.

The analogy to the Hopf bifurcation in the circle model is striking: The quasi-stationary solutions become convectively unstable for $\alpha := V'(h_f) > \alpha_c$ where α_c is some critical value. Numerical experiments and the study of the spectrum of an infinite matrix let us conjecture that $\alpha_c = \alpha^H = 0.5$. Fig. 4 shows an example where $\alpha = 0.645 > \alpha_c$. The perturbation ($\dot{x}_1(0) = v_c < v_f$) is propagating upstream with increasing amplitudes. The opposite occurs in Fig. 5, where $\alpha = 0.331 < \alpha_c$. Here the perturbations have decreasing amplitudes. Further experiments are presented in Sec. 2.1.

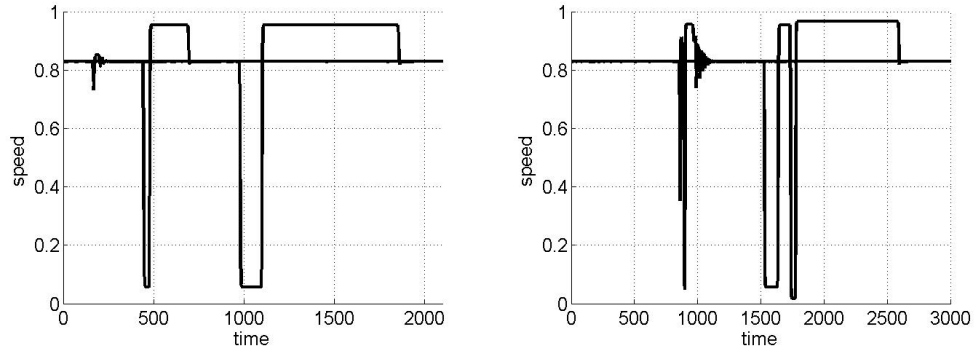

(a) cars No. 100, 300 and 700

(b) cars No. 500 and 1000

Figure 6: Two different jam waves for $h_f = 1.4, \varrho_f = 0.714, \alpha = 0.57$: Time-speed functions of different cars with different initial perturbations

Our numerical analysis consists essentially of two parts. In the first part (Sec. 2.1) we investigate the convective stability of the quasi-stationary solutions by imposing a small perturbation $\dot{x}_1(0) = c \cdot v_f$ to the leading car with $c \approx 1, c \neq 1$. Some results are presented in Fig. 13 and Fig. 14. They confirm the conjecture that $\alpha_c = \alpha^H$. This implies that the quasi-stationary solutions are convectively unstable for $\varrho_{f,1} = 0.69 < \varrho_f < \varrho_{f,2} = 1.81$ respectively for $h_{f,1} = 1.45 > h_f > h_{f,2} = 0.55$. We call the densities $\varrho_{f,j}$ **critical densities** and the corresponding headways $h_{f,j}$ **critical headways** $(j = 1, 2)$. They seem to coincide with the Hopf bifurcation parameters in the circle model.

In the second part (Sec. 2.2)we want to know which kinds of propagating (traveling) waves (called **jam waves**) show up, especially when the quasi-stationary solutions are unstable. Of course, this depends on the initial perturbations. One type of waves which are very similar to the traveling waves in the circle model (see [Wer11]) occur for headways h_f in the neighborhood of the critical headways $h_{f,j}, j = 1, 2$, especially in the region of coexistence with stable quasi-stationary solutions. Fig. 6(a) shows the evolution of a jam wave for $h_f = 1.4$. Here, a single car, not too close to the top of the autocade, runs through different phases which are characterized by certain (headway, speed)-pairs $(h_f, v_f), (h_{min}, v_{min}), (h_{max}, v_{max})$ and (h_f, v_f) again, where h_{min} is very small, $v_{min} = V(h_{min})$, and $h_{max} > h_f$, $v_{max} = V(h_{max})$. Fig. 6(a) indicates that the time a single car needs to pass the two interesting phases (h_{min}, v_{min}) (the jam phase), and (h_{max}, v_{max}) (the non-jam phase) increases with the distance to the leading car. One can say that the jam wave runs through different quasi-stationary phases.
For the same parameters, we have also found jam waves with two jam phases of different depths for another initial perturbation, see Fig. 6(b), where also the time a single car remains in the jam, seems to increase with the distance to the leading car.

There is a rich variety of jam waves we have found in our numerical experiments, see Sec. 2.2 and Fig. 7 which shows the time-speed functions of single cars. In addition to that, Fig. 8 presents another visualizations of the jam waves, by looking at the speed of the whole car ensemble at some specific time T.

We did not only find jam waves for those parameters where the quasi-stationary solutions are unstable, but also for those where stable quasi-stationary solutions coexist, comparable to Fig. 3 for the circle model. In coincidence with this model we conjecture that the **magic headways** $h_1 = 0.1441, h_2 = 1.8559$ we have found in [Wer11] have the following meaning for the line model: For $h_f < h_1$ and for $h_f > h_2$ the only long term attractors are the quasi-stationary solutions. All up and downs caused by the initial perturbation will eventually vanish while traveling upstream. For $h_1 < h_f < h_2$ there exist jam waves which may be rather simple (as in Fig. 7(a) for $h_f = 1.6$) or somehow chaotic (see Fig. 16(e) for $h_f = 1.20$). The jam fronts seem to travel with constant speed, at least concerning the jam front, which a single car hits the first time for $h_f > 1.1$. With increasing time, the jam areas become larger.

Comparing Fig. 7(b) and Fig. 7(e) we discover a symmetry phenomenon, possibly due to the same value of α and the point symmetry of the optimal velocity function $V(h)$ with respect to $h = 1$. Somehow the figures are complementary to each other. While the first one, for $h_f = 1.4$, shows a jam wave with a short dramatic jam phase, the second one, for $h_f = 0.6$, shows a jam wave with a short non-jam phase. The first figure is more interesting since the traffic density here is much smaller than in the second figure. In most parts of the paper we limit our experiments to the parameter region $h_f > 1$ of smaller density ϱ_f.

1.2 Introduction: Movies

The video format of the following videos is *mp4*. You need a player on your computer which can handle this format. The movies show speed configurations of the whole car ensemble as function of time (compare with Fig. 8 for a fixed time). Initially, the perturbation of the quasi-stationary solution is described by two parameters n_c and h_c: At time $t = 0$, the first n_c cars have all speed $v_c = V(h_c) < v_f$, while all other cars start with the quasi-stationary pair (h_f, v_f), $v_f = V(h_f)$.
In the movie of Fig. 9, we have $h_f = 1.6$. Due to the fact that the quasi-stationary solution is convectively stable for this parameter value, $h_c = 1.1$ has to be chosen much smaller than h_f to let the dynamics converge against a coexisting jam wave.
For the parameter $h_f = 1.4$ in Fig. 10, the quasi-stationary solution is unstable. The convergence of the dynamics against a jam wave can be observed already for $h_c = 1.3$ — a rather small perturbation of h_f. The same situation is shown in Fig. 11-12. In all these movies we assume $n_c = 10$.
The red point indicates the place where cars are entering the jam area the first time. From the movies one can guess that the jam speed is constant and that it decreases with increasing h_f.

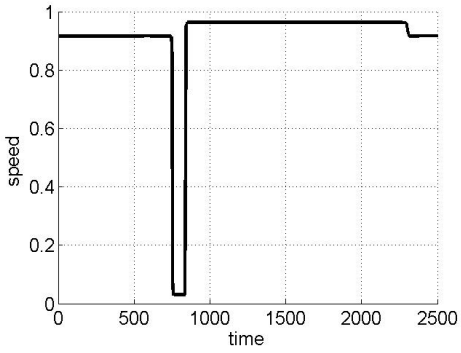

(a) $h_f = 1.6, \varrho_f = 0.625, \alpha = 0.31$

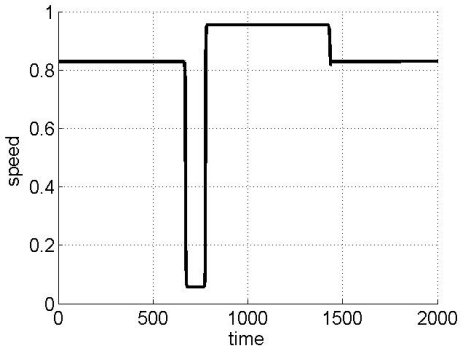

(b) $h_f = 1.4, \varrho_f = 0.714, \alpha = 0.57$

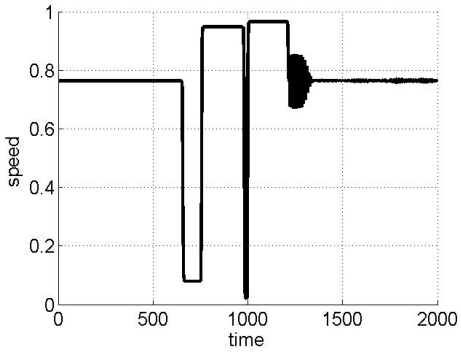

(c) $h_f = 1.3, \varrho_f = 0.77, \alpha = 0.73$

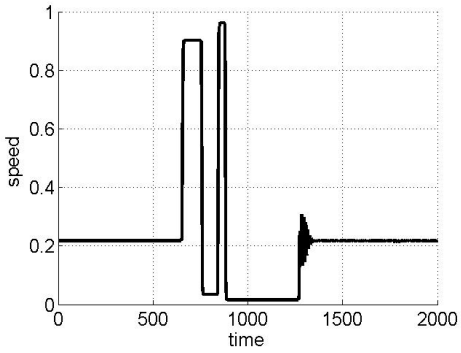

(d) $h_f = 0.7, \varrho_f = 1.43, \alpha = 0.72$

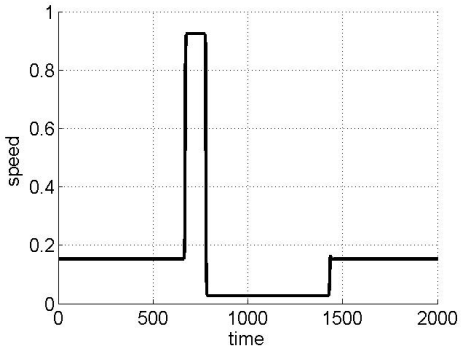

(e) $h_f = 0.6, \varrho_f = 1.67, \alpha = 0.57$

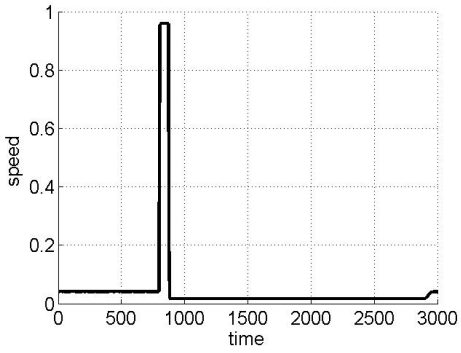

(f) $h_f = 0.3, \varrho_f = 3.33, \alpha = 0.22$

Figure 7: Time-speed functions of car No. 500 for different densities.

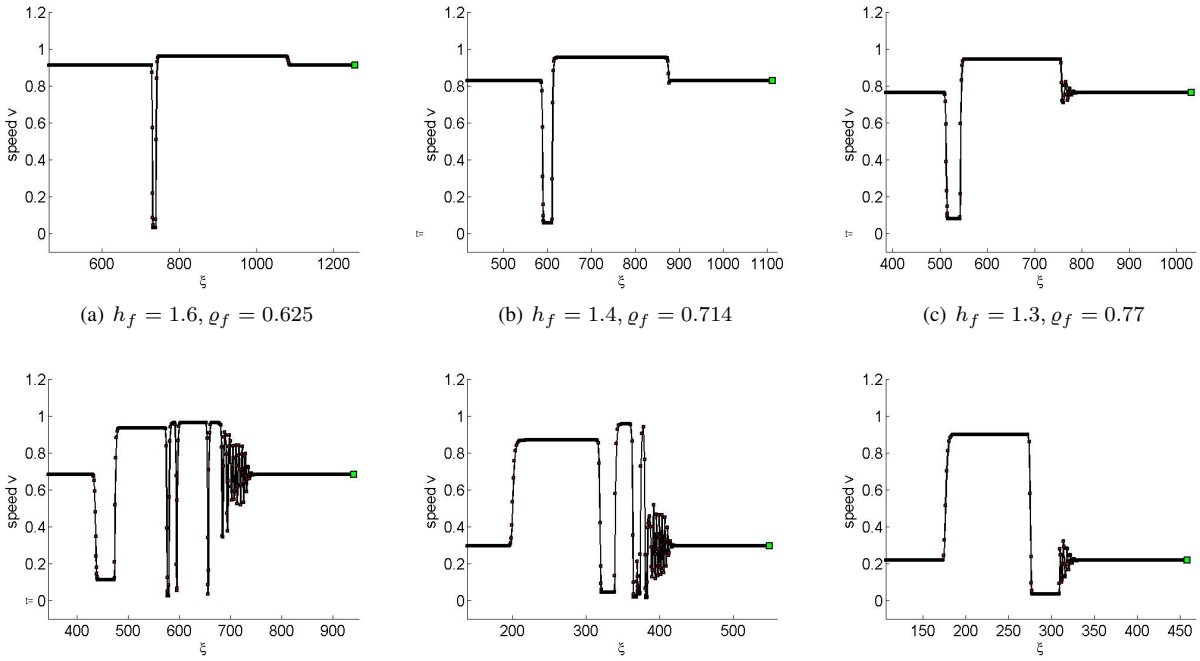

(a) $h_f = 1.6, \varrho_f = 0.625$ (b) $h_f = 1.4, \varrho_f = 0.714$ (c) $h_f = 1.3, \varrho_f = 0.77$

(d) $h_f = 1.2, \varrho_f = 0.83$ (e) $h_f = 0.8, \varrho_f = 1.25$ (f) $h_f = 0.7, \varrho_f = 1.43$

(g) $h_f = 0.6, \varrho_f = 1.67$ (h) $h_f = 0.3, \varrho_f = 3.33$

Figure 8: The speed configurations of the whole car ensemble at time $T = 500$ for different h_f.

(Loading moviehf1,6hc1,1nc10.mp4)

Figure 9: Movie: $h_f = 1.6, h_c = 1.1, n_c = 10$

(Loading moviehf1,4hc1,3nc10.mp4)

Figure 10: Movie: $h_f = 1.4, h_c = 1.3, n_c = 10$

(Loading moviehf1,3hc1,2nc10.mp4)

Figure 11: Movie: $h_f = 1.3, h_c = 1.2, n_c = 10$

(Loading moviehf1,2hc1,1nc10.mp4)

Figure 12: Movie: $h_f = 1.2, h_c = 1.1, n_c = 10$

1.3 Introduction: Some Theory

The concept of convective instability makes sense only for the infinite ODE system (4). This system has a special triangular structure: The dynamics of car No. N is determined by an N-dimensional ODE system. For a rigorous analytical approach we need a theory for infinite ODE systems in analogy to the finite ones (existence, uniqueness, stability, principle of linearized stability). First of all we need a suitable Banach space. In Sec. 3 we investigate the spectrum of the linearization at the equilibrium. We get desirable results if we let the infinite matrix operate on ℓ_2. Therefore we believe that ℓ_2 is the right Banach space — after some transformation which transforms the equilibrium given by h_f and v_f to zero. But we will not try a rigorous approach here.

Numerically, we investigate (in)stability of the quasi-stationary solutions by allowing only perturbations in a finite part at the top of the autocade, especially by a single perturbation $\dot{x}_1(0) \neq v_f$ of the leading car. This leads to a slightly weaker concept of stability than the usual one, which carries over to the infinite ODE system where perturbations of infinite many cars would be taken into account. Instead of that we will perform certain numerical stability tests in Sec. 2.1 observing how perturbations will travel upstream.

We believe that some principle of linearized stability holds. Linearizing the infinite headway-speed system along the quasi-stationary equilibrium we obtain an infinite linear ODE system

$$\dot{x} = A_\infty(\alpha)x \tag{5}$$

with an infinite triangular block matrix

$$A_\infty(\alpha) := \begin{pmatrix} D(\alpha) & O & O & O & \dots \\ C & D(\alpha) & O & O & \dots \\ O & C & D(\alpha) & O & \dots \\ \vdots & \ddots & \ddots & \ddots & \ddots \end{pmatrix}. \tag{6}$$

and

$$D(\alpha) := \begin{pmatrix} 0 & -1 \\ \alpha & -1 \end{pmatrix}, \quad C = \begin{pmatrix} 0 & 1 \\ 0 & 0 \end{pmatrix}$$

depending on $\alpha = V'(h_f)$.
The finite principal $N \times N$-part $A_N(\alpha)$,

$$A_N(\alpha) := \begin{pmatrix} D(\alpha) & O & O & O & \dots & O \\ C & D(\alpha) & O & O & \dots & O \\ O & C & D(\alpha) & O & \dots & O \\ \vdots & \ddots & \ddots & \ddots & \ddots & \vdots \\ O & \dots & O & C & D(\alpha) & O \\ O & \dots & O & O & C & D(\alpha) \end{pmatrix}.$$

determines the stability of the finite N-car autocade. The only eigenvalues of $A_N(\alpha)$ are two geometrically simple (!!) eigenvalues

$$\lambda_{1,2}(\alpha) := -\frac{1}{2} \pm \sqrt{\frac{1}{4} - \alpha}$$

with algebraic multiplicity N.

Numerical experiments with this infinite linear and the nonlinear system (see Sec. 2.1) show that the principle of linearized instability seems to hold — for $\alpha > \alpha_c = \alpha^H = 0.5$ the trivial solution seems to be unstable as well as the quasi-stationary solution. Another numerical experience is that the trivial solution of the linear systems as well as the quasi-stationary solution is weakly stable for $\alpha < \alpha^H$ - another indication that some linearized stability holds.

Analytically, it is obvious to investigate the spectrum $\sigma(A_\infty)$ in dependence of the parameter α. Indeed, in Sec. 3 we determine the spectrum of $A_\infty(\alpha)$ and show that $\alpha > \alpha^H$ if and only if there are continuous spectral values with positive real part while for $\alpha < \alpha^H$ the spectrum is contained in the left half complex plane including the value zero.

2 Numerical results

2.1 Instability test for the quasi-stationary solutions

The simplest perturbation of the quasi-stationary solution is given by the initial choice $\dot{x}_1(0) \neq v_f$ for the leading car while all the other initial conditions are left unchanged ($\dot{x}_{j+1}(0) = v_f, x_j(0) - x_{j+1}(0) = h_f, j = 1, 2, ...$). We want to show instability of the quasi-stationary solution if $\alpha = V'(h_f) > \alpha^H := 0.5$ or equivalently if $0.55 < h_f < 1.45$, respectively if $0.69 < \varrho_f < 1.81$. We choose $\dot{x}_1(0) = 0.9v_f$, hoping that this perturbation will reveal instability.
For a given N and a given time t we compute the euclidean distance

$$d_N(t) := \Big(\sum_{j=1}^{N} (\dot{x}_j(t) - v_f)^2 + (h_j(t) - h_f)^2 \Big)^{1/2}, \; h_j := x_j - x_{j+1},$$

of the N-car autocade state to the quasi-stationary state. We draw the graph of $d_N(t)$ as function of time and diagnose instability if this graph has an obvious tendency to increase for sufficiently large N and t.
Fig. 13 and 14 show some graphs of $d_N(t)$ for different values of h_f and N. They impressively justify our guess concerning instability. But note that we need very large values of N and of t to detect instability for values of α only slightly larger than $\alpha^H = 0.5$.
Stability cannot be so clearly diagnosed by this technique which uses a very simple single perturbation. But it is tempting to conclude stability from Fig. 13(h) for $h_f = 1.45$ and $\alpha = 0.496 < \alpha^H$.

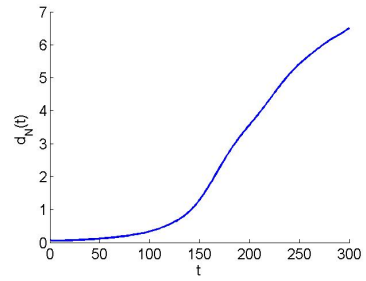

(a) $h_f = 1.3, \alpha = 0.725, N = 300$

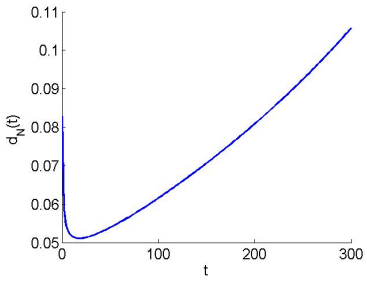

(b) $h_f = 1.4, \alpha = 0.569, N = 300$

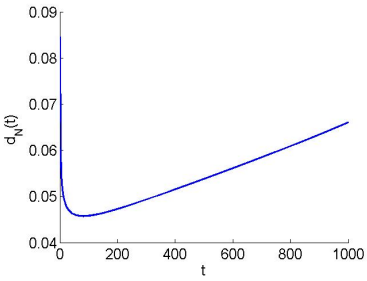

(c) $h_f = 1.43, \alpha = 0.525, N = 1000$

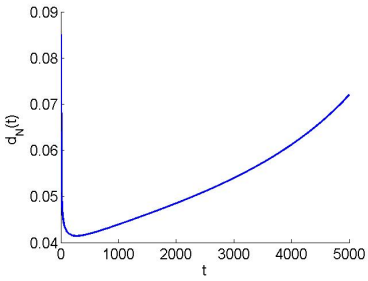

(d) $h_f = 1.44, \alpha = 0.510, N = 5000$

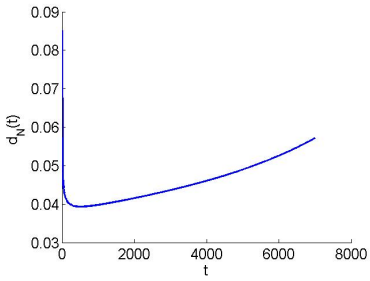

(e) $h_f = 1.443, \alpha = 0.5058, N = 7000$

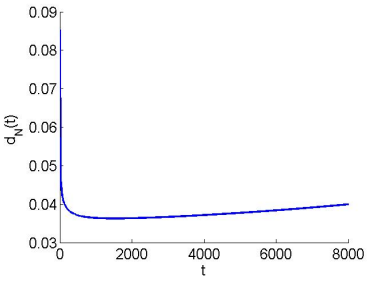

(f) $h_f = 1.446, \alpha = 0.5015, N = 8000$

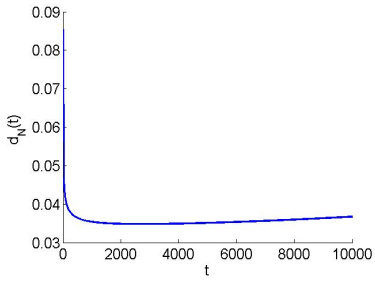

(g) $h_f = 1.447, \alpha = 0.5001, N = 10000$

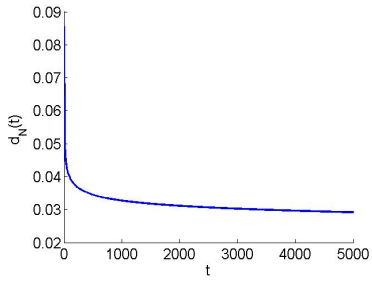

(h) $h_f = 1.45, \alpha = 0.496, N = 5000$

Figure 13: Numerical test of convective stability: Graph of $d_N(t)$ ($h_f \in [1.30, 1.45]$)

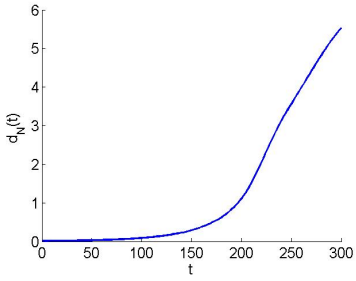

(a) $h_f = 0.70, \alpha = 0.725, N = 300$

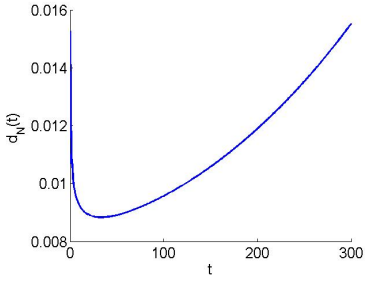

(b) $h_f = 0.60, \alpha = 0.569, N = 300$

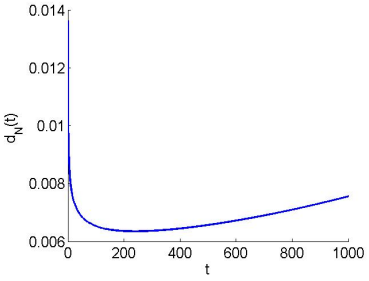

(c) $h_f = 0.57, \alpha = 0.525, N = 1000$

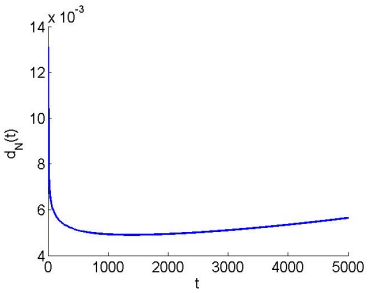

(d) $h_f = 0.56, \alpha = 0.510, N = 5000$

Figure 14: Numerical test of convective stability ($h_f \in [0.56, 0.70]$): Graph of $d_N(t)$

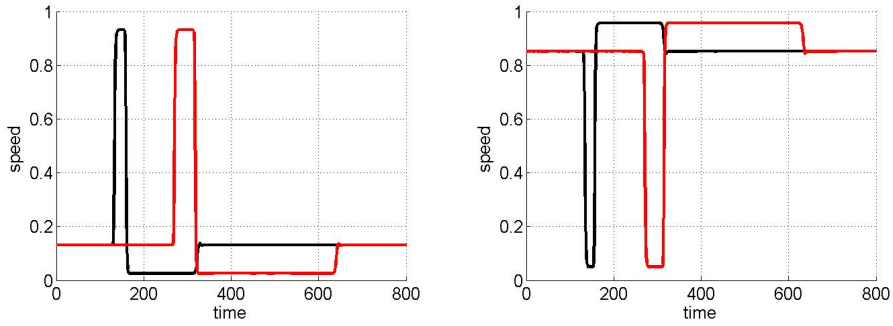

(a) $h_f = 0.56, \alpha = 0.510$ (b) $h_f = 1.44, \alpha = 0.510$

Figure 15: Jam wave: Speed dynamics of single cars No. 100 (black) and car No. 200 (red) as function of time for $h_f = 0.56$ and $h_f = 1.44$.

2.2 Jam waves

In Sec. 2.1 we have tested the convective instability of the quasi-stationary solutions by imposing very small, very special perturbations. Now we are going to find out the type of evolving solutions when the quasi-stationary solutions are unstable ($0.55 < h_f < 1.45$). Fig. 16 presents some results by plotting the speed of certain cars as function of time. Initially, at time $t = 0$, the quasi-stationary solution are perturbed slightly by requiring speed v_c and headway h_c with $V(h_c) = v_c$ for the first n_c cars. We always choose $n_c = 3$.

We have to distinguish the cases $h_f < 1$ (large density) and $h_f > 1$ (small density). This is reflected by our choice of $h_c = 1/h_f$. The results for these two cases are somehow inverse symmetric to each other due to the point symmetry of the optimal velocity function. This is demonstrated impressively by Fig. 15.
Fig. 15(a) for $h_f = 0.56$ can be obtained from Fig. 15(b) for $h_f = 1.44$ by point reflection (note that in both cases $\alpha = V'(h_f) = 0.51$). In the first one, a car is always caught in a jam with a short exceptional time when the car runs fast. This symmetry holds in all other computations.
Our jam experiences on motorways let us feel familiar with situations like in Fig. 15(b) for smaller densities ($h_f = 1.44$) where each car has to pass a dramatic, but relatively short jam phase. Since we are mainly interested in such cases ($h_f > 1$) we we will present the following numerical results only for smaller densities. A theoretical foundation of this observed point symmetry is not in the focus of this paper.

The first observation from Fig. 16 is the almost rectangular structure with significant wave fronts evolving for $1.3 \leq h_f \leq 1.45$, at least when the cars hit the jam front the first time. We call these solutions **jam waves**. Fig. 17 presents the corresponding macro visualizations from which one can conclude that the speed of the jam front is constant, at least the speed of the first front a car is hitting. We call the speed of this front **jam speed**. It decreases with increasing headway h_f (and hence with decreasing traffic density ϱ_f).
Observe that the jam area increases with time. The farther away from the top, the longer a car stays in the jam. This can be concluded from the jam cones in Fig. 17. The smaller the traffic density, the smaller the angle of the cone.

Fig. 17 is more suitable to visualize the traveling wave dynamics of the autocade as to plot the speed of single cars as function of time. Other better insights in the traveling wave dynamics are the movies presented in Sec. 1.2 or the speed configuration of the whole car ensemble as in Fig. 8.

Our numerical experience indicates the stability of the quasi-stationary solutions iff $\alpha < 0.5$ ($h_f > h_1^H = 1.45$ or $h_f < h_2^H = 0.55$). Now we are going to study the coexistence of stable quasi-stationary solutions with jam waves which evolve if the initial state does not belong to the domain of attraction of the corresponding stable quasi-periodic solution.

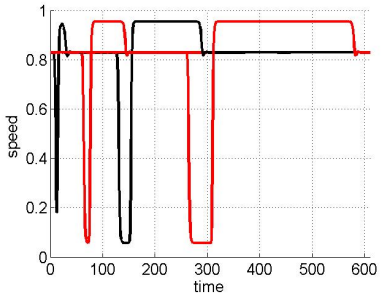

(a) $h_f = 1.40, \alpha = 0.569$

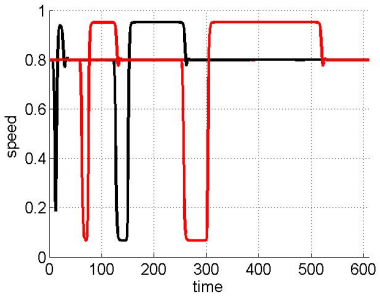

(b) $h_f = 1.35, \alpha = 0.646$

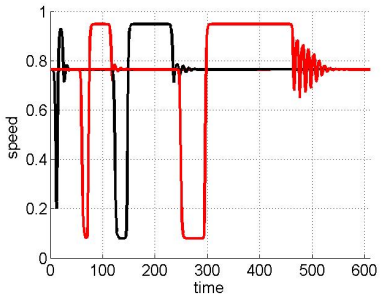

(c) $h_f = 1.30, \alpha = 0.725$

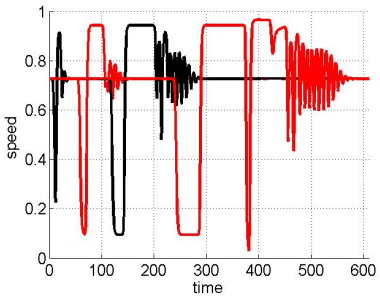

(d) $h_f = 1.25, \alpha = 0.800$

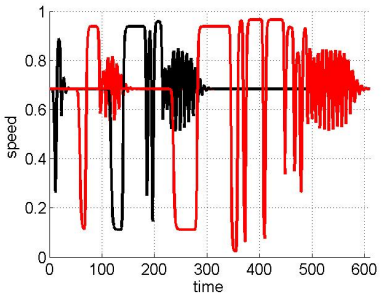

(e) $h_f = 1.20, \alpha = 0.871$

Figure 16: Speed v of car No. 10 (black), No. 50 (red), No. 100 (black), No. 200 (red) as function of time for different h_f with unstable quasi-stationary solutions ($\alpha > 0.5$)

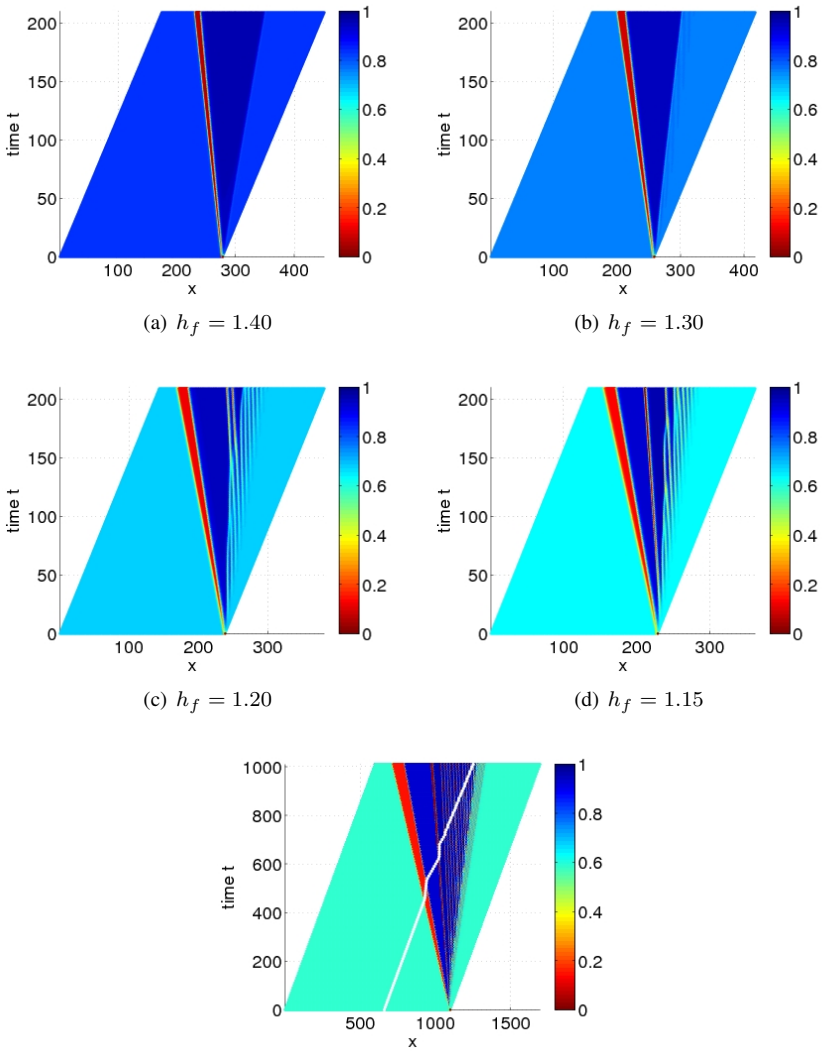

(a) $h_f = 1.40$

(b) $h_f = 1.30$

(c) $h_f = 1.20$

(d) $h_f = 1.15$

(e) $h_f = 1.10$ with trajectory of car No. 500

Figure 17: Macro visualization of the speed for different h_f

By suitable initial states, we obtain jam waves for $h_f \in [1.5, h_2]$, $h_2 := 1.8559$ with the same simple structure as in Fig. 16(a) for $h_f = 1.40$, see Fig. 18. Here h_2 is the magic headway mentioned in the Introduction and introduced in [Wer11] for the circle model. For $h_f > h_2$ the jams were eventually dying away — the jam pattern is only a transient event. For $h_f = h_2$ the jam area remains constant, the minmal headway in the jam is the other magic headway $h_1 = 1.441$.

2.3 Conclusions

What do we conclude from the numerical experiments?

1. As in the circle model, the (convective) stability of the quasi-stationary solution depends only on $\alpha = V'(h_f)$.
2. The critical bifurcation parameter where stability is lost is $\alpha_c = 0.5$, which coincides with the Hopf bifurcation parameter α^H in the circle model.
3. In the headway (density) parameter setting there are two bifurcation points where the quasi-stationary solution looses stability. The two critical headways $h_j, j = 1, 2$ are given by $V'(h_j) = 0.5$ and have the approximate numerical values
$$h_1 = 0.55, \quad h_2 = 1.45.$$
The quasi-stationary solutions are unstable for headways $h \in [h_1, h_2]$. The corresponding critical densities are $\varrho_1 = 1/h_1 = 1.81$ and $\varrho_2 = 1/h_2 = 0.69$. These critical parameters are the same as in the circle model.
4. When the quasi-stationary solutions are unstable, some traveling waves called jam waves evolve. The first jam front travels upstream with constant speed.
5. For small densities ($h_f > 1.3$) there are jam waves with rectangular structure very similar to the periodic traveling waves in the circle model. But in general, the jam area changes size with time.
6. For middle sized densities ($1 < h_f < 1.25$) there are jam waves which are rather chaotic with rapid changes between fast and slow speeds.
7. Jam waves coexist with stable quasi-stationary solutions for the same densities (headways) as in the circle model.

3 Theory

We recall from the Introduction (Sec. 1.3) that the linearization of the infinite nonlinear traffic model leads to an infinite linear ODE system involving the infinite triangular matrix

$$A_\infty(\alpha) := \begin{pmatrix} D(\alpha) & O & O & O & \dots \\ C & D(\alpha) & O & O & \dots \\ O & C & D(\alpha) & O & \dots \\ \vdots & \ddots & \ddots & \ddots & \ddots \end{pmatrix}.$$

with

$$D(\alpha) := \begin{pmatrix} 0 & -1 \\ \alpha & -1 \end{pmatrix}, \quad C = \begin{pmatrix} 0 & 1 \\ 0 & 0 \end{pmatrix}.$$

Numerically we have observed stability for $\alpha < 0.5$ and instability for $\alpha > 0.5$. Here (in)stability is understood in the sense of the (in)stability of the equilibrium of the nonlinear infinite ODE system or (an equivalent numerical observation) as the (in)stability of the trivial solution of the infinite ODE system $\dot{x} = A_\infty(\alpha)x$ in a suitable Banach space which we believe should be chose as ℓ_2 being the space of all complex sequences equipped with the 2-norm.

We are interested in the **spectrum** of $A_\infty(\alpha)$, and we will show that for $\alpha > 0.5$ there is a continuum of spectral values with positive real part. The proof may be of interest also without the traffic background.

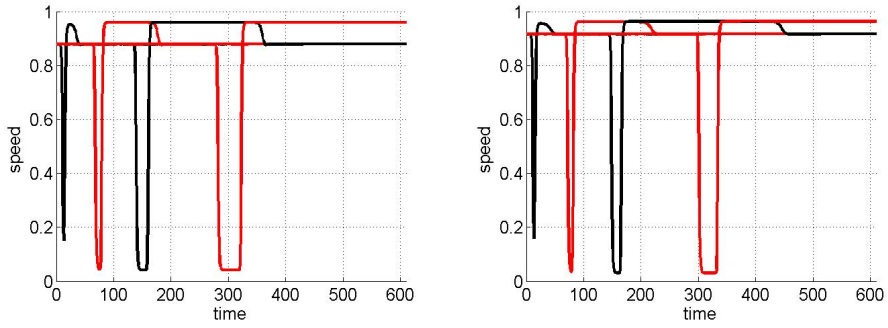

(a) $h_f = 1.50, \alpha = 0.428$ (b) $h_f = 1.60, \alpha = 0.311$

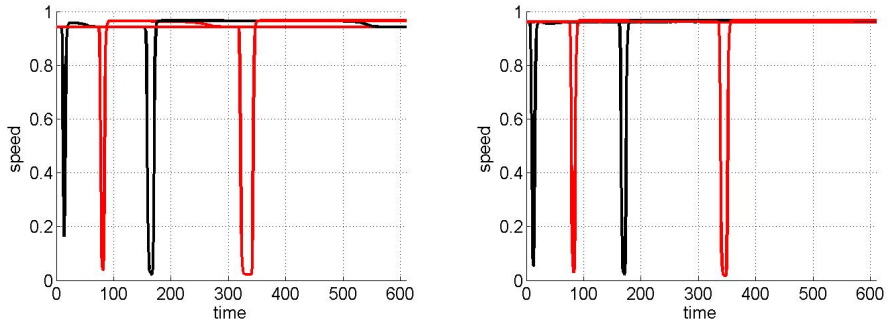

(c) $h_f = 1.70, \alpha = 0.220$ (d) $h_f = 1.80, \alpha = 0.153$

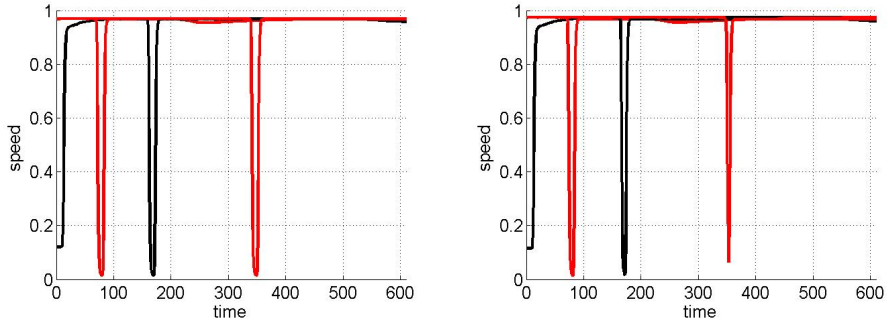

(e) $h_f = 1.85, \alpha = 0.127$ (f) $h_f = 1.90, \alpha = 0.105$

Figure 18: Speed v of car No. 10 (black), No. 50 (red), No. 100 (black), No. 200 (red) as function of time for different h_f with stable quasi-stationary solutions ($\alpha < 0.5$)

The finite principal $N \times N$-part

$$A_N(\alpha) := \begin{pmatrix} D(\alpha) & O & O & O & \dots & O \\ C & D(\alpha) & O & O & \dots & O \\ O & C & D(\alpha) & O & \dots & O \\ \vdots & \ddots & \ddots & \ddots & \ddots & \vdots \\ O & \dots & O & C & D(\alpha) & O \\ O & \dots & O & O & C & D(\alpha) \end{pmatrix}.$$

determining the stability of the quasi-stationary solution of a finite N-car autocade is highly non-normal, and there is a guess that its pseudospectrum is related to the spectrum $\sigma(A_\infty(\alpha))$.
We do not follow this line suggested by TILMAN SELIG[3]. Instead we consider a slight perturbation of $A_N(\alpha)$, leading to the circulant matrix

$$A_{N,\circ}(\alpha) := \begin{pmatrix} D(\alpha) & O & O & O & \dots & C \\ C & D(\alpha) & O & O & \dots & O \\ O & C & D(\alpha) & O & \dots & O \\ \vdots & \ddots & \ddots & \ddots & \ddots & \vdots \\ O & \dots & O & C & D(\alpha) & O \\ O & \dots & O & O & C & D(\alpha) \end{pmatrix},$$

which appears in a related stability analysis of a N-car-traffic model on a circle ([GSW04]). As shown in this paper, this model undergoes a Hopf bifurcation for $\alpha = \alpha_N := \frac{1}{1+c_N}$, where $c_N := \cos(2\pi/N)$. It can be shown that $i \cdot \omega_N$ is an eigenvalue of $A_{N,\circ}(\alpha_N)$ with $\omega_N := \frac{s_N}{1+c_N}$ and $s_N := \sin(2\pi/N)$. Observe that $\alpha_N \to 0.5$ for $N \to \infty$ which may be the key for our stability observation. [GSW04] contains a slightly more general result: For each number $k = 1, 2, ..., \lfloor N/2 \rfloor$ there are Hopf bifurcations for

$$\alpha = \alpha_{k,N} := \frac{1}{1 + c_{k,N}}, \quad c_{k,N} := \cos(2k\pi/N)$$

with imaginary eigenvalues

$$i \cdot \omega_{k,N}, \quad \omega_{k,N} = \alpha_{k,N} s_{k,N}, s_{k,N} := \sin(2\pi/N).$$

For our investigations it is remarkable that for fixed k, we have $\alpha_{k,N} \to 0.5$ and $\omega_{k,N} \to 0$ for $N \to \infty$.

The key point of our result is that the set $\sigma(A_{N,\circ}(\alpha))$ of all eigenvalues of $A_{N,\circ}(\alpha)$ is a subset of $\sigma(A_\infty(\alpha))$. Hence the last remark indicates that our observed bifurcation in the infinite ODE-traffic model might be related to a highly degenerated Hopf bifurcation of infinite dimension.

Before we will prove the key role of $A_{N,\circ}(\alpha)$, it might be worthwhile to look at Fig. 19 showing how the eigenvalues of $A_{N,\circ}(\alpha)$ depend on α for different N. We focus on α in the neighborhood of $\alpha = 0.5$.

We start our analysis with the simple fact that $A_\infty(\alpha)$ is a bounded linear operator on ℓ_2. We are interested in the spectrum $\sigma(A_\infty(\alpha))$ in this setting. For $y \in \ell_2$ we define $y_N \in \mathbb{C}^{2N}$ to be the first N block components of y.
We note that $(A_\infty(\alpha)y)_N = A_N(\alpha)y_N$. From here it follows that

$$((A_\infty(\alpha) - \lambda I)y)_N = A_N(\alpha)y_N - \lambda y_N$$

and that $A_\infty(\alpha)$ has no eigenvalues.
We remark that the construction of a sequence y_n in ℓ_2 such that $\|y_n\| = 1$ and $\|A_\infty(\alpha)y_n - \lambda y_n\| \to 0$ for $n \to \infty$ implies $\lambda \in \sigma(A_\infty(\alpha))$. Such λ-values are called **generalized eigenvalues**.

Theorem: All eigenvalues of $A_{N,\circ}(\alpha)$ and their accumulation points for an arbitrary N belong to the spectrum of $A_\infty(\alpha)$.

[3]Department of Mathematics, Technical University of Ilmenau

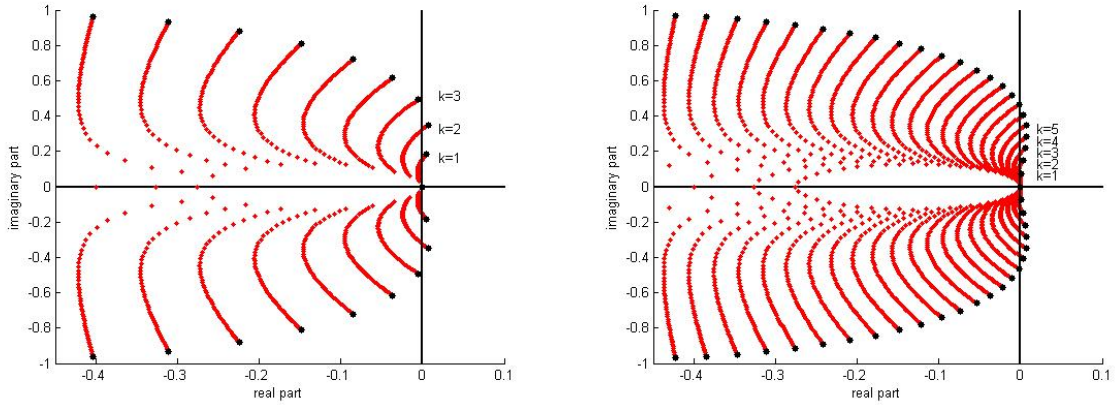

(a) $N = 20$ (b) $N = 50$

Figure 19: Eigenvalues of $A_{N,\circ}(\alpha)$ in dependence on $\alpha = 0.1, ..., 0.6$

Proof: The structure of eigenvalues and eigenvectors of $A_{N,\circ}(\alpha)$ is very simple. Let λ_N be an eigenvalue of $A_{N,\circ}(\alpha)$. The corresponding eigenvector can be assumed to have the following circulant structure: $y := (y_1, ..., y_N)$ with $y_j \in \mathbb{C}^2$ and $y_{j+1} = \gamma_N y_j$ where γ_N is an Nth root of unity. It follows easily that λ_N is an eigenvalue of

$$B(\alpha, \gamma) := \begin{pmatrix} 0 & -1 + \frac{1}{\gamma} \\ \alpha & -1 \end{pmatrix}$$

with $\gamma = \gamma_N$ We claim that

$$G(\alpha) := \{\lambda \in \mathbb{C} : \lambda \in \sigma(B(\alpha, \gamma)) \text{ for } \gamma \in \mathbb{C}, |\gamma| = 1\} \subset \sigma(A_\infty(\alpha)) \tag{7}$$

Let $\lambda \in G(\alpha)$. Then there is a sequence $(N_n)_{n\in\mathbb{N}}$ with $N_n \to \infty$ such that $\lambda_{N_n} \in G(\alpha)$ is an eigenvalue of $A_{N_n,\circ}$ and $\lambda_{N_n} \to \lambda$ for $n \to \infty$ [4]. Now set $N = N_n$ for simplicity. The corresponding eigenvector $y^N \in \mathbb{C}^{2N}$ can be prelonged by zeros to a vector in ℓ_2. Also $A_{N,\circ}(\alpha)$ can be considered as an operator on ℓ_2 by adding an infinite number of zero blocks. Denote the infinite vector and matrix again by y^N and $A_{N,\circ}(\alpha)$ respectively. Then

$$\|A_\infty(\alpha)y^N - \lambda_N y^N\| \le \|A_\infty(\alpha)y^N - A_{N,\circ}(\alpha)y^N\| + \|A_{N,\circ}(\alpha)y^N - \lambda_N y^N\|. \tag{8}$$

Since the last term in (8) vanishes, we are finished if $\|A_\infty(\alpha)y^N - A_{N,\circ}(\alpha)y^N\|$ tends to zero for $n \to \infty$ (then $N = N_n \to \infty$).
But

$$d_N := A_\infty(\alpha)y^N - A_{N,\circ}(\alpha)y^N$$

is zero except Cy_N^N in the first and in the $(N+1)$th block components, where $y_N^N \in \mathbb{C}^2$ is the Nth component of y^N. On the other hand because of $y_{j+1}^N = \gamma_N y_j^N$ with $\gamma_N^N = 1$ (an Nth root of unity), all $\mathbb{C}^2$-components $y_j^N, j = 1, 2, ..., N$ have the same 2-norm. Since we can assume that $\|y^N\| = 1$, we have $\|y_N^N\| = \frac{1}{\sqrt{N}}$. Hence $\|A_\infty(\alpha)y^N - A_{N,\circ}(\alpha)y^N\|$ tends to zero and we are finished. □

Obviously $\sigma(A_{N,\circ}(\alpha)) = G_N(\alpha)$ where

$$G_N(\alpha) := \{\lambda \in \mathbb{C} : \lambda \in \sigma(B(\alpha, \gamma_N)) \text{ with } \gamma_N^N = 1\} \subset G(\alpha).$$

[4] This is also true for eigenvalues $\lambda \in \sigma(A_{N,\circ}(\alpha))$ and fixed $N := N_0$, since λ is also an eigenvalue of $A_{N,\circ}(\alpha)$ for all multiples of N_0.

Since $|1/\gamma| = 1$ if $|\gamma| = 1$ we can replace $B(\alpha, \gamma)$ by

$$B(\alpha, \gamma) := \begin{pmatrix} 0 & -1+\gamma \\ \alpha & -1 \end{pmatrix}.$$

The eigenvalue equation for an eigenvalue of $B(\alpha, \gamma)$ is very simple:

$$\lambda(\lambda + 1) + \alpha(1 - \gamma) = 0.$$

If λ is a solution, then also $-\lambda - 1$. Hence $G(\alpha)$ is point-symmetric with respect to $\lambda = -0.5$. It is very easy to draw $G(\alpha)$, see Fig. 20 and Fig. 21. The pictures are very similar to those of the pseudo spectra of $A_N(\alpha)$, see Fig. 22, obtained by the Matlab tool *eiglib*. This is not surprising since $A_{N,\circ}(\alpha)$ can be considered as a small perturbation of $A_N(\alpha)$ where only one 2×2-zero-block is replaced by C.

Remark: A more general result seems to hold: $G(\alpha)$ is not only contained in the set of generalized eigenvalues of $A_\infty(\alpha)$ — there are no other ones. The main argument for this is the fact that for $\lambda \notin G(\alpha)$ the resolvent $(A_{N,\circ}(\alpha) - \lambda I)^{-1}$ is uniformly bounded[5], since

$$((A_\infty(\alpha) - \lambda)y)_N = (A_N(\alpha) - \lambda)y_N = (A_N(\alpha) - A_{N,\circ}(\alpha))y_N + (A_{N,\circ}(\alpha) - \lambda)y_N =: u_N + v_N.$$

Assume that $y \in \ell_2$ satisfies $\|y\| = 1$ and $\|(A_\infty(\alpha) - \lambda)y\| \le \varepsilon$ for some $\lambda \notin G(\alpha)$. Then for sufficiently large N we have $\|y_N\| \ge 1 - \varepsilon$, $\|u_N\| \le \varepsilon$ and $\|v_N\| \le \varepsilon$. This contradicts the uniform boundedness of $(A_{N,\circ}(\alpha) - \lambda I)^{-1}$.

The residual spectrum of $A_\infty(\alpha)$ contains the two eigenvalues $\lambda_{1,2}(\alpha) := -\frac{1}{2} \pm \sqrt{\frac{1}{4} - \alpha}$ of $A_N(\alpha)$. The arguments are as follows: λ is in the residual spectrum iff there is $y \neq 0$ being orthogonal to the range of $A_\infty(\alpha) - \lambda I$. Let $y_1 \in \mathbb{C}^2$ be the left eigenvector of $D(\alpha)$ associated with $\lambda_j, j = 1$. Choose $y \in \ell_2$ with vanishing block-components except the first one chosen as y_1. Then $y^H(A_\infty(\alpha) - \lambda_1 I) = 0$ because of the triangular structure of $A_\infty(\alpha)$. Hence λ_1 is in the residual spectrum of $A_\infty(\alpha)$. The same holds for $\lambda = \lambda_2$
Let $\lambda \neq \lambda_j, j = 1, 2$, be in the residual spectrum and let $y = (y_1, y_2, ..., ..) \neq 0$ with $\mathbb{C}_2$-block components be orthogonal to the range of $A_\infty(\alpha) - \lambda I$. Then $y_1^H(D(\alpha) - \lambda I) = 0$. Hence $y_1 = 0$ which implies $y_2^H(D(\alpha) - \lambda I) = 0$, etc ...

By our Theorem we have proved that the quasi-stationary solution of an infinite autocade is unstable for $\alpha > 0.5$ provided that the principle of linearized stability holds for the infinite ODE system. The stability for $\alpha < 0.5$ is not proved by this Theorem because of the fact that for all α zero is an accumulation point of spectral values. But from the last remark we follow that there are no spectral values of $A_\infty(\alpha)$ having positive real part if $\alpha < 0.5$. The numerical observation of stability for $\alpha < 0.5$ was associated with a very slow convergence. The reason may be the generalized eigenvalue zero.

[5] This has been tested numerically, not yet proven.

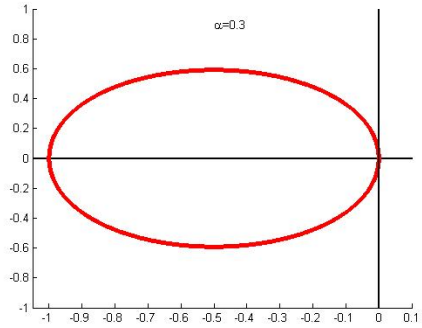

(a) $\alpha = 0.3$

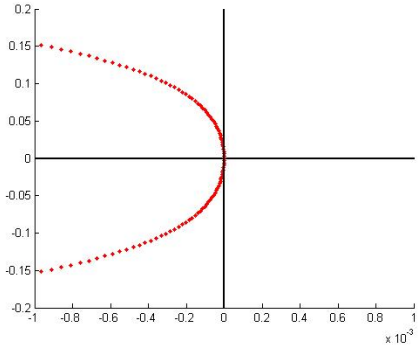

(b) $\alpha = 0.49$

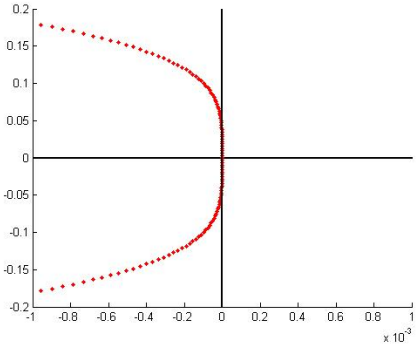

(c) $\alpha = 0.5$

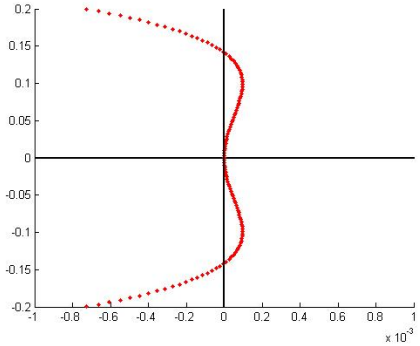

(d) $\alpha = 0.51$

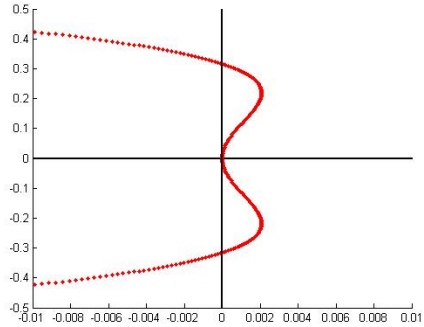

(e) $\alpha = 0.55$

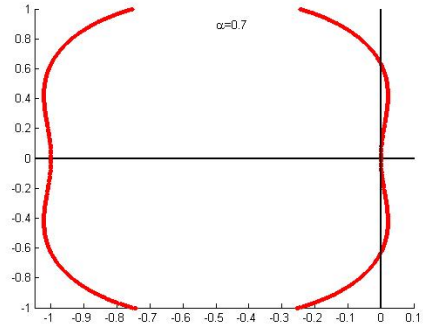

(f) $\alpha = 0.7$

Figure 20: Subsets of the spectrum of $A_\infty(\alpha)$ for different values of α

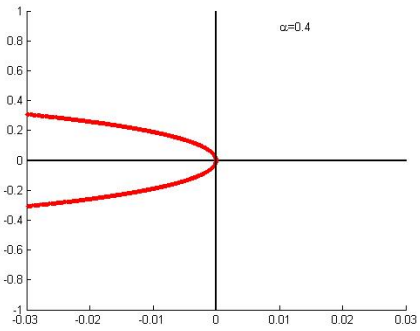

(a) $\alpha = 0.4$

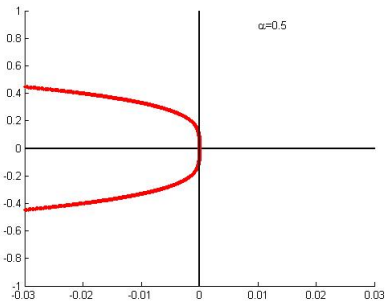

(b) $\alpha = 0.5$

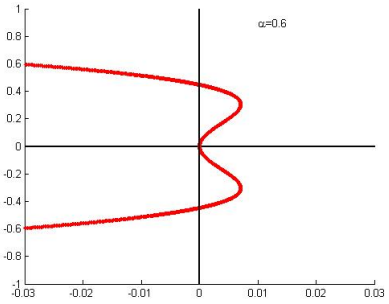

(c) $\alpha = 0.6$

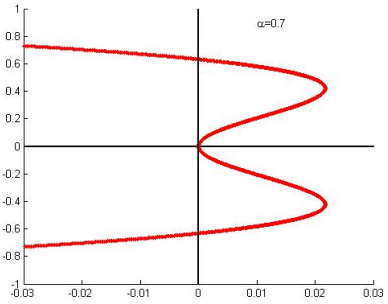

(d) $\alpha = 0.7$

Figure 21: The spectrum of $A_\infty(\alpha)$ near the imaginary axis for different values of α.

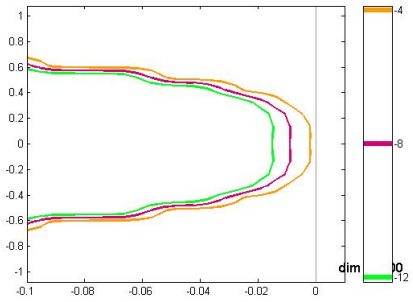

(a) $\alpha = 0.5$

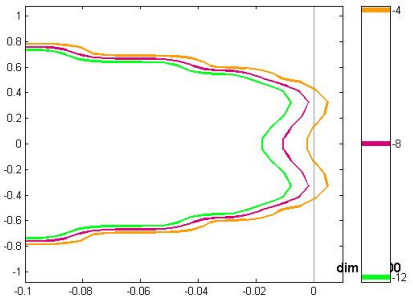

(b) $\alpha = 0.6$

Figure 22: Pseudo spectrum of $A_N(\alpha)$ for $N = 800$

References

[BHN+95] M. Bando, K. Hasebe, A. Nakayama, A. Shibata, and Y. Sugiyama. Dynamical model of traffic congestion and numerical simulation. *Phys. Rev. E*, 51:1035ff, 1995.

[GSW04] I. Gasser, G. Sirito, and B. Werner. Bifurcation analysis of a class of 'car following' traffic models. *Physica D*, 197/3-4:222–241, 2004.

[GW10] I. Gasser and B. Werner. Dynamical phenomena induced by bottleneck. *Phil. Trans. R. Soc. A 368, 4543-4562*, 2010.

[SGW09] T. Seidel, I. Gasser, and B. Werner. Microscopic car-following models revisited: from road works to fundamental diagrams. *SIAM J. Appl. Dyn. Sys. 8, 1305-1323*, 8 (3):1305–1323, 2009.

[Wer11] B. Werner. An asymptotic numerical analysis of hopf periodic traveling waves for a microscopic traffic problems. *Hamburger Beiträge zur Angewandten Mathematik*, 2011.